Building Tomorrow's Society

*Bâtir la Société de Demain*

Fredericton, Canada

June 13 – June 16, 2018/ *Juin 13 – Juin 16, 2018*

# MECHANICS-BASED ANALYSIS MODEL FOR SLENDER MASONRY WALLS

Pettit, Clayton[1], Cruz-Noguez, Carlos[2,4] and Hagel, Mark[3]
[1] University of Alberta, Canada
[2] University of Alberta, Canada
[3] Alberta Masonry Council, Canada
[4] cruznogu@ualberta.ca

**Abstract:** A slender masonry wall is currently defined by the Canadian guidelines for masonry structures (CSA S304-14) to have a slenderness ratio greater or equal to 30. Slender walls are an attractive structural option for low-rise construction, such as warehouses, school gymnasiums, and retail stores due to their low construction costs. The code provisions for slender walls are based on observations from experimental programs dealing with these slender walls, basic principles of mechanics of materials, and practical considerations arising from masonry workmanship. However, due to the difficulties in studying walls with high slenderness, very few experimental tests dealing with masonry walls with slenderness ratios greater than 30 have been conducted and in turn, aspects of the structural response of these slender masonry walls are still not well understood. Such aspects include the effective stiffness at failure, deformation, stability, safety limits on the axial loads that these walls can carry, and the influence of the grouting extent (i.e., fully grouted walls vs. partially grouted walls). In consequence, the code provisions have led to an uneconomical masonry solution in comparison with competing for construction alternatives, such as wood and steel. In this study, a simplified, yet robust analysis model for masonry walls based on basic mechanics of materials is developed. The model implements a fibre-section approach to account for the nonlinearity of the masonry and reinforcement materials in the moment-curvature response. Second-order effects are integrated into the model by solving the pertinent differential equations that govern the deformation of beam-columns. The analysis model will be validated with experimental tests conducted by ACI-SEASC Task Committee on Slender Walls. The limitations of the model are discussed, and design recommendations have been provided.

## 1 INTRODUCTION

Canadian guidelines classify a slender masonry wall as a wall having a slenderness ratio greater or equal to 30. Although slender masonry walls are desirable for low-rise construction such as gymnasium walls or warehouses, they are particularly susceptible to second-order effects. Design codes have provisions to determine the magnitude of second-order effects, but due to the nonlinearities of masonry materials and the difficulty in testing slender masonry walls, the variation of effective stiffness as loading is applied is not well understood. This has led to inaccurate estimations of slender wall deflections using current design code equations.

Finite element (FE) methods have been used to analyze slender masonry walls (Liu and Dawe 2002). FE models account for the variation of effective stiffness of slender walls under loading, resulting in greater

accuracy over design codes in approximating deflections. However, FE analysis is time-consuming and expensive. In this study, a mechanics-based parametric analysis is proposed as an alternative. Mechanics-based analysis models for slender elements under axial load have previously been developed and applied to prestressed concrete columns (Nathan 1985) through column deflection curves (CDC). While CDCs applies only to elements with equal end moments under single curvature bending, Newmark's Numerical Method was later applied to include elements under double curvature (Muqtadir 1991). The application of CDCs to slender masonry walls is presented in the current study, and its performance and limitations are discussed.

## 2 ANALYSIS MODEL

### 2.1 Formulation

Consider the deflection curves of a pinned-pinned masonry wall as illustrated in Figure 1.

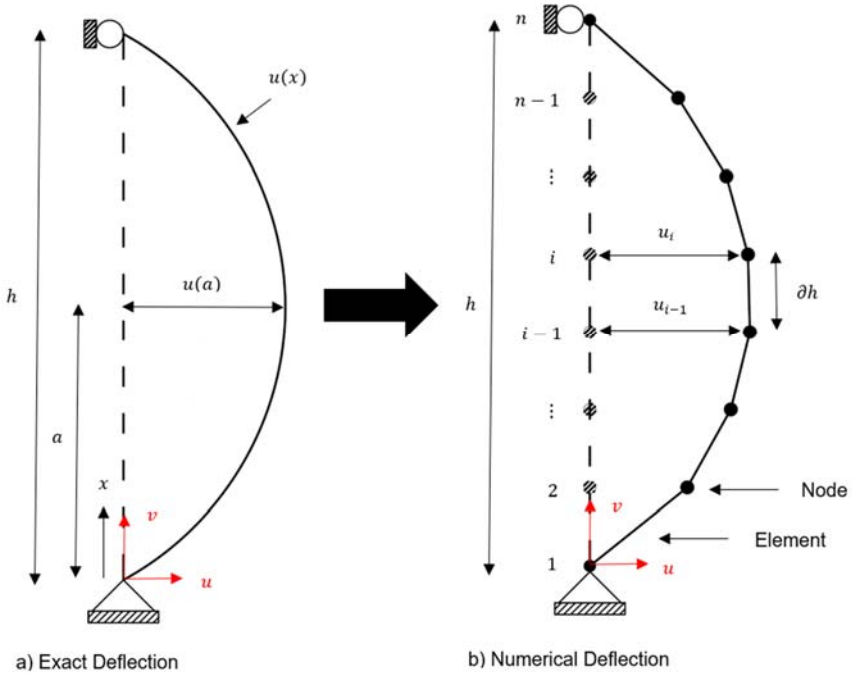


Figure 1: Deflection Curves for Masonry Walls

For the deflection curve seen in Fig. 1(a) a function ($u(x)$) can be defined used to determine the horizontal deflection at any point ($x$) along the height of the wall. This function is obtained through solving the differential equation (Timoshenko and Gere 1961) shown below (Eq. 1).

[1] $\frac{\partial^2}{\partial h^2}\left(EI\frac{\partial^2 u}{\partial h^2}\right) + P\frac{\partial^2 \mathrm{u}}{\partial h^2} = q(x)$

Where

$h$ = The height of wall

$EI$ = The effective stiffness of the wall

$u$ = The deflection of the wall

$P$ = The axial load placed on the wall

$q(x)$ = The distributed lateral load placed along the height of the wall

Due to the cracking of the masonry under tensile loads and the nonlinearity of the constitutive relationships for steel and masonry, the effective stiffness term ($EI$) in Eq. 1 is not constant. Therefore, an exact solution of Eq. 1 is complex and difficult to determine. The solution of Eq. 1 can be approximated by a Taylor Series expansion (Eq. 2) as

[2] $u(x) = u(a) + \frac{u'(a)}{1!}(x-a) + \frac{u''(a)}{2!}(x-a)^2 + \cdots$

Where

$u(x)$ = The value of the deflection function at point $x$

$u(a)$ = The value of the deflection function at point $a$

$u'(a)$ = The value of the deflection functions first derivative at point $a$

$u''(a)$ = The value of the deflection functions second derivative at point $a$

$(x-a)$ = The distance between points $x$ and $a$

Equation (2) indicates that the horizontal deflection at any point ($x$) along the masonry wall may be determined if the parameters of another point ($a$) are known. Equation 2 can also be further simplified using the relationships between deflection, slope and curvature shown below:

[3] $u'(x) = \alpha(x)$

[4] $u''(x) = \phi(x)$

Where

$\alpha(x)$ = The slope at point $x$

$\phi(x)$ = The curvature at point $x$

If the wall is discretized into $n-1$ elements connected by $n$ nodes, a piecewise deflection curve can be used to approximate the exact deflection of the wall as illustrated in Fig. 1(b). Assuming the parameters of node $i-1$ are known, a Taylor Series expansion (Eq. 2) can be used to approximate the horizontal deflection at node $i$:

[5] $u_i = u_{i-1} + \alpha_{i-1}\partial h + \frac{1}{2}\phi_{i-1}\partial h^2$

Where

$u_i$ = The deflection at node $i$

$u_{i-1}$ = The deflection at node $i-1$

$\alpha_{i-1}$ = The slope at node $i-1$

$\phi_{i-1}$ = The curvature of node $i-1$

$\partial h$ = The distance between nodes $i$ and $i-1$ (The length of the element)

Thus, to determine the deflection at each node, the deflection, slope, and curvature at the previous node must be known. A relationship for slope between nodes $i$ and $i-1$ can be determined using a similar methodology:

[6] $\alpha_i = \alpha_{i-1} + \phi_{i-1}\partial h$

Where

$\alpha_i$ = The slope at node $i$

The curvature of each node is determined by equating the external moment to the internal moment (both depicted in Fig. 2) as expressed below:

[7] $M_{ext,i} = M_{int,i}$

Where

$M_{ext,i}$ = The external moment at node $i$

$M_{int,i}$ = The internal moment at node $i$

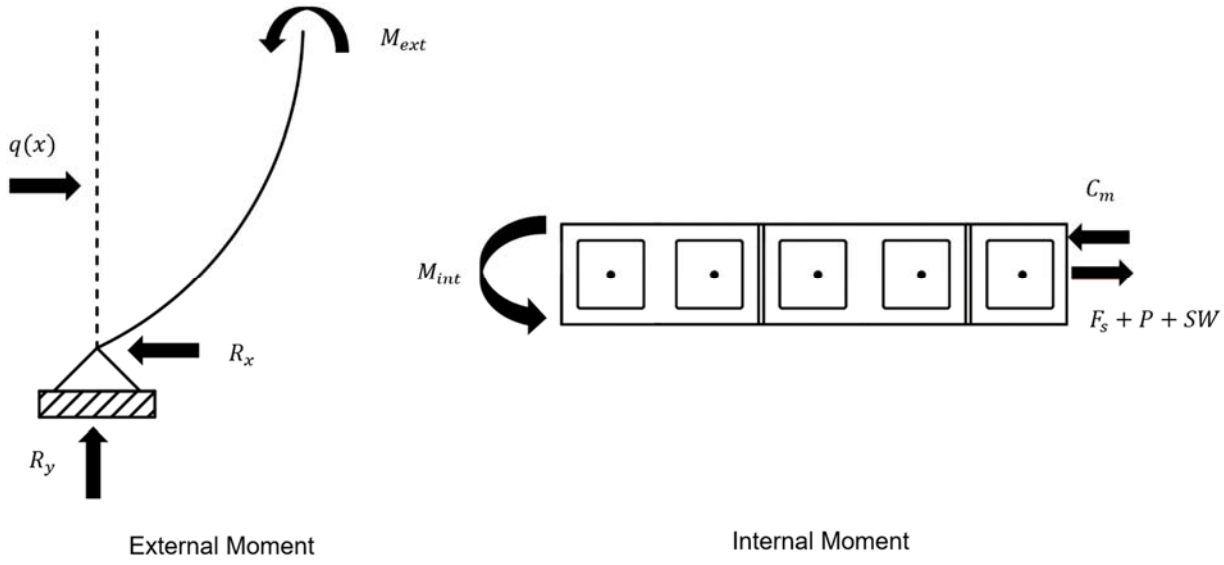


Figure 2: External and Internal Moments

Referring to Fig. 2, the external moment at a node can be determined using statics. Both first- and second-order effects must be considered; first-order moments are caused by lateral loads and concentrated moments, while second-order moments are caused by the deflection of the wall producing an eccentricity associated with the axial load acting on the wall. The total external moment of a node can be determined through:

[8] $M_{ext,i} = M_{o,i} + (P + SW_i)\left(u_{i-1} + \frac{\alpha_{i-1}\partial h}{2}\right)$

Where

$M_{o,i}$ = The first order moment at node $i$

$SW_i$ = The self-weight of the masonry above node $i$

Once the internal moment at a node is known, the associated value of curvature can be obtained through a conventional section compatibility analysis (a suitable algorithm is discussed in the next section).

The analysis model described above was implemented in a script using MATLAB (MATLAB 2016).

### 2.2 Moment-Curvature Relationship

A moment-curvature relationship is developed using strain compatibility. The cross-section is discretized into fibres. Material properties and geometry of the fibres are used to determine the forces present in each fibre for different values of strain (Figure 4) using suitable constitutive relationships. Once equilibrium is satisfied, the resisting moment can be obtained by taking the moment of the forces in the fibres about a

reference axis (e.g., the outermost fibre in compression, Eq. 9) and the curvature can be obtained by dividing the outermost compressive stresses of the masonry by the depth of the neutral axis (Eq. 10), as follows:

[9] $M_{int} = \sum C_{mi} d_i + \sum T_{mi} d_i + \sum F_{si} d_i + (P + SW)\left(\frac{t}{2}\right)$

[10] $\phi = \frac{\epsilon}{N.A.}$

Where

$M_{int}$ = The resisting moment of the section (internal moment)

$C_{mi}$ = The compressive force of the masonry in fibre $i$

$T_{mi}$ = The tensile force of the masonry in fibre $i$

$F_{si}$ = The force in steel bar $i$

$d_i$ = The distance from fibre $i$ to the reference axis

$t$ = The thickness of the masonry unit

$\phi$ = The curvature of the section

$\epsilon$ = The strain of the outmost fibre in compression

$N.A.$ = The neutral axis of the section

The ultimate moment and curvature correspond either to the point in which the masonry crushes (Figure 3) in compression or when the rupture of the steel is reached.

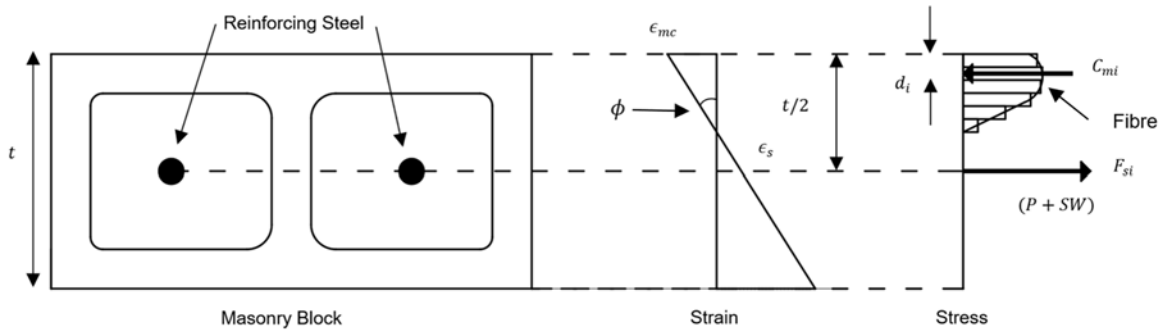


Figure 3: Moment and Curvature at Ultimate

The location of the neutral axis is determined through an iterative procedure in which equilibrium (Eq. 11) is checked in the cross-section.

[11] $\sum C_{mi} + \sum T_{mi} + \sum F_{si} + P + SW = 0$

### 2.3 Masonry and Steel Material Models

To simulate the response of masonry material under compression, a modified version the model proposed by (Priestley and Elder 1983) has been chosen. This model assumes the maximum stress of the masonry to occur at a strain of 0.002 (Drysdale and Hamid 2005). The behavior of steel is assumed to be an elastic plastic material with strain hardening.

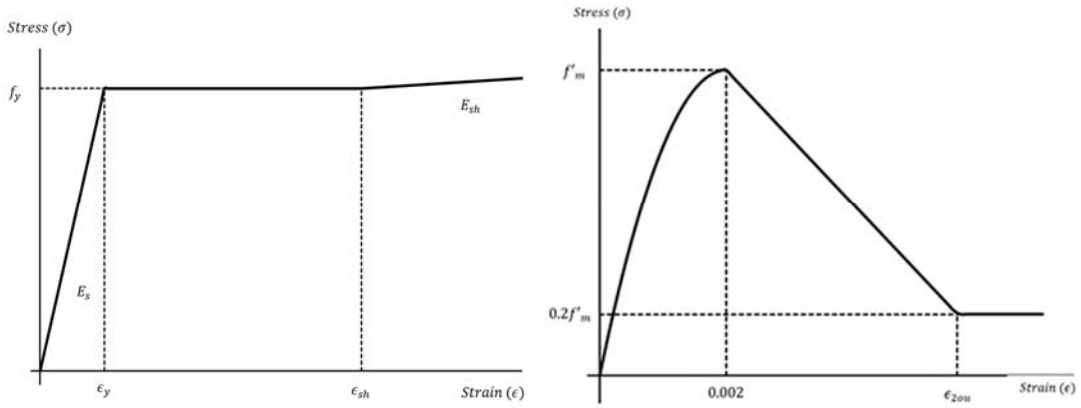


Figure 4: Constitutive relationships for steel (left) and masonry (right)

## 3 VALIDATION

Test results of slender masonry walls conducted by the ACI-SEASC Task Committee on Slender Walls (ACI-SEASC 1982) are utilized to verify the model. The walls were tested using an airbag that applied uniform pressure on one side of the wall (Fig. 5). This pressure was increased until either failure or judgment that failure was near. Each wall also carried an eccentric axial load. The mid-wall displacement and lateral pressure were recorded at intervals during the experiment.

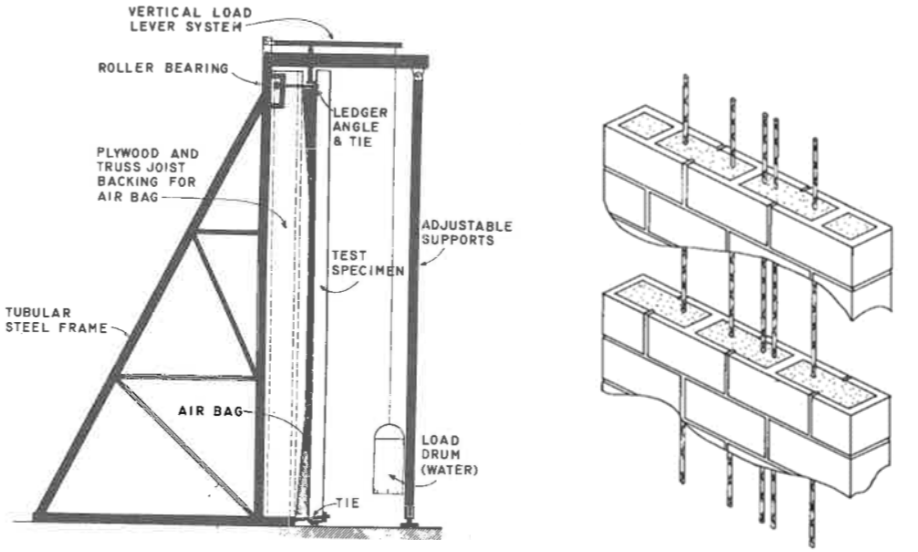


Figure 5: Testing Mechanism of the Masonry Walls (ACI-SEASC 1982)

### 3.1 Masonry Wall Assemblage

Results for 9 masonry walls panels are available. Different thicknesses of concrete masonry units used for the panels were 6'' [143.0mm], 8'' [193.8mm] and 10'' [246.1mm]. Material properties of the units were determined on site through prism testing. Geometric and material properties of the walls are shown in Tables 1 and 2 respectively.

Table 1: Masonry Wall Panel Geometry

| Panel | Panel Thickness (mm) | Axial Load (kN) | Slenderness Ratio | Failure Mode |
|---|---|---|---|---|
| 1 | 246.1 | 5.7 | 30.6 | Stopped Test |
| 2 | 246.1 | 15.3 | 30.6 | Stopped Test |
| 3 | 246.1 | 15.3 | 30.6 | Stopped Test |
| 4 | 193.8 | 15.3 | 38.8 | Stopped Test |
| 5 | 193.8 | 15.3 | 38.8 | Stopped Test |
| 6 | 193.8 | 5.7 | 38.8 | Stopped Test |
| 7 | 143.0 | 5.7 | 52.6 | Masonry Crushing |
| 8 | 143.0 | 5.7 | 52.6 | Masonry Crushing |
| 9 | 143.0 | 5.7 | 52.6 | Stopped Test |

Table 2: Masonry Material Properties

| Masonry Unit | Compressive Strength (MPa) | Modulus of Elasticity (MPa) |
|---|---|---|
| 10'' [246.1mm] | 16.96 | 14962 |
| 8'' [193.8mm] | 17.89 | 11859 |
| 6'' [143.0mm] | 21.96 | 10963 |

Each panel was reinforced with five bars of Grade 60 [420 MPa] steel (Fig. 5). Material properties of the steel rebar are shown in Table 3.

Table 3: Steel Rebar Properties

| Grade | Yield Strength (MPa) | Ultimate Strength (MPa) | Yield Strain | Youngs Modulus (MPa) |
|---|---|---|---|---|
| 60 | 483 | 758 | 0.0025 | 197190 |

### 3.2 Results

For the initial pre-cracked, elastic response, the analytical model predicts an accurate load-displacement response in the elastic region for each panel.

After cracking, but before yielding, the model predicts greater deflections than those obtained during the experimental results, for the same levels of lateral loads. The discrepancy is more prevalent in the 10'' [246.1mm] panels than with the 6'' [143.0mm] panels. The analytical predictions for panels 1, 4, and 8 closely resemble the behavior of the experimental tests with only minor variations. Analytical predictions for panel 2, 3, 5, 6, 7 and 9, however, appear to overestimate the stiffness of the panels as the slope of their load-displacement curve is slightly higher than those from experimental results.

After yielding, analytical load-displacement responses predict a large amount of deflection over small increases of lateral pressure. Although this behavior is present in the experimental results as well, the slope of the load-displacement response of the experimental results is slightly higher than the analytical predictions. This is especially present in panel 4 where this is a noticeable difference in slope after yielding between experimental and analytical results. When approaching the ultimate moment of the panels, many of the analytical results for the panels predict a greater failure displacement than the experimental results with the exceptions being panels 3, 7 and 8. This behavior is expected as experimental testing of the panels (except for panels 7 and 8) was stopped before failure occurred. Investigating both panels 7 and 8, the failure point predicted by the analytical model and that of the experimental results match well. The failure lateral pressure predicted by the analytical model also approximates that of the experimental testing for the remaining panels suggesting the analytical model retains a reasonable level of accuracy.

Graphs representing the lateral pressure as a function of midpoint deflection for all panels can be found in Fig. 6.

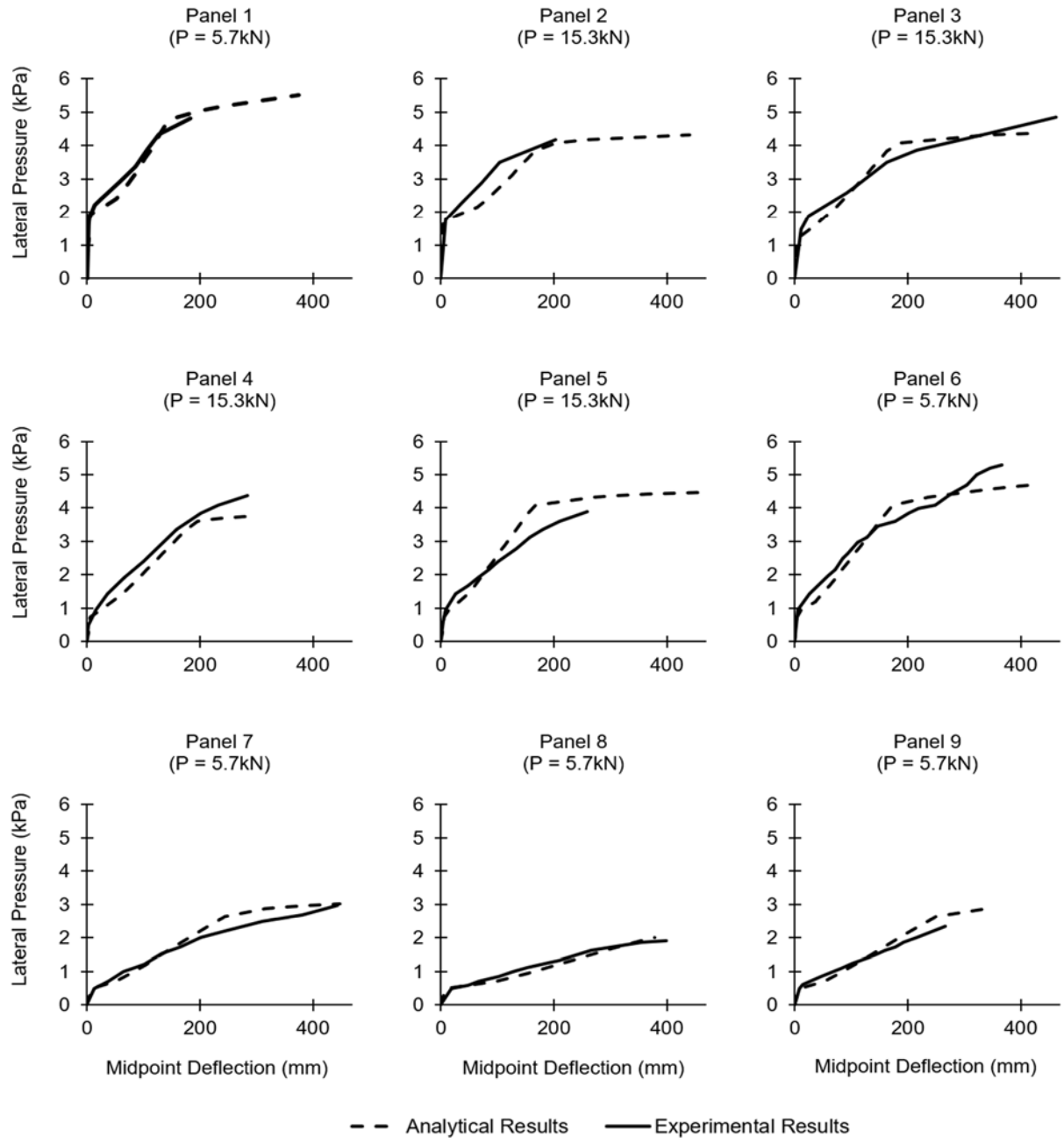


Figure 6: Experimental to Analytical Comparison

## 4 APPLICATIONS

### 4.1 Interaction Diagram with Slenderness Consideration

Slenderness interaction diagrams can be used to determine any combination of axial load and moment placed on a wall before failure occurs. Without the inclusion of slenderness, the failure mode of masonry walls governed by material failure (e.g. the masonry crushing or steel fracturing). However, as the slenderness increases, the failure mode is governed by stability (e.g. the buckling of the wall).

To generate a slenderness interaction diagram for a masonry wall, a constant axial load is placed atop the wall. The eccentricity of this load will be varied until the wall has reached failure. This process is iterated for various levels of axial load until enough points are determined to construct the curve (Fig. 7). It is observed that as the slenderness of the wall increases, the axial load and moment capacity significantly decreases.

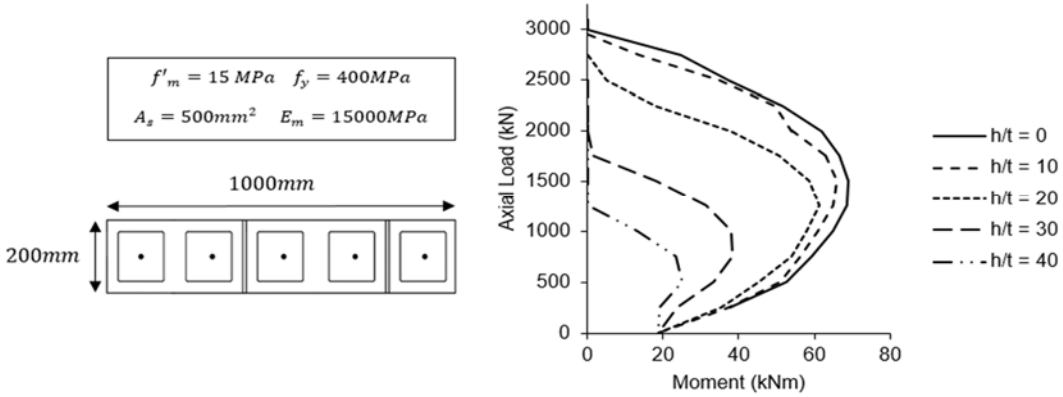


Figure 7: Slenderness Interaction Diagram

### 4.2 Comparison to the Canadian Standard

To demonstrate the conservatism of the Canadian standard for masonry structures (S304-14), both the experimental and analytical results of Panel 3 have been compared with the deflection obtained with the current design equations. As seen, the design equations predict much more deflection under the same loads as compared to both analytical and experimental results under service conditions.

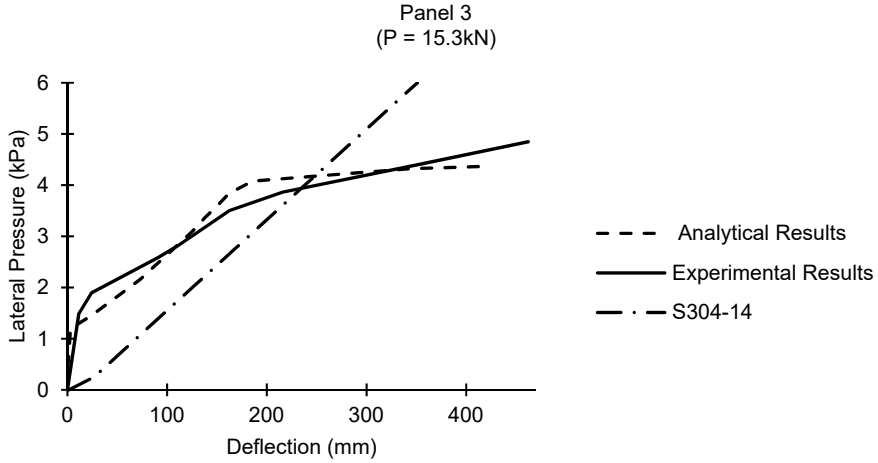


Figure 8: Comparison to Canadian Design Equation

### 4.3 Model Limitations

The process outlined above is only valid for single curvature masonry walls with simple boundary conditions.

## 5 CONCLUSION

Due to the nonlinearities of masonry materials and the difficulty in testing slender masonry walls, the effective stiffness of a masonry wall under loading is not well understood, resulting in difficulty estimating the true horizontal deflection. As the effective stiffness is a key term in the differential equation governing the deflection of beam-column elements, solving this equation becomes quite complex. As an alternative, a mechanics-based algorithm has been presented to solve this differential equation numerically through the segmentation of a masonry wall into a finite number of nodes and elements. A fibre-section approach is used to account for the nonlinearity of the masonry and reinforcement materials in the moment-curvature response. The procedure is easily programmable into spreadsheets, leading to a quick and effortless way to analyze the behavior of slender masonry walls. In addition, aspects such as the changing effective stiffness, second-order effects, and failure modes can be determined under multiple loading scenarios. The validity of the model has been verified with test results conducted by the ACI-SEASC Task Committee on Slender Walls and the current limitations of the algorithm are presented.

### Acknowledgements

The authors would like to give special thanks to Dr. Yong Li of the University of Alberta for all the technical support given in the development of the program. The authors would also like to recognize the gracious support of both the Alberta Masonry Council (AMC) and Masonry Contractors Association of Alberta (MCAA).

### References

ACI-SEASC Task Committee on Slender Walls, “Test Report on Slender Walls”, American Concrete Institute and the Structural Engineers Association of Southern California, February 1980 - September 1982, Los Angeles.

Abdul Muqtadir, Mohammad. 1991. “Slenderness Effects in Eccentrically Loaded Masonry Walls.” Ph.D. diss. University of Alberta.

CSA S304, 2014. *Design of masonry structures.* 2 edn. Mississauga, Canada: Canadian Standards Association.

Drysdale, R.G. and Hamid, A.A. 2005. *Masonry Structures: Behavior and Design.* Englewood Cliffs, NJ.

Liu, Yi. 2002. “Beam-Column Behavior of Masonry Structural Elements.” Ph.D. diss. University of New Brunswick.

MATLAB. 2016. Natick, MA: The MathWorks, Inc.

Moosavi Nanehkaran, Seyed Abdol Hadi. 2016. “Structural reliability of Non-slender loadbearing concrete masonry members under concentric and eccentric loads.” Ph.D. diss. University of Alberta.

Nathan, N. 1985. Rational Analysis and Design of Prestressed Concrete Beam Columns and Wall Panels. *PCI Journal.* May-June 1985, PCI.

Priestley, M and Elder, D. 1983. Stress-strain curves for unconfined and confined concrete masonry. *ACI Journal Proceedings* 1983, ACI.

Yimoshenko, Stephen, James Gere. *Theory of Elastic Stability,2nd Edition.* McGraw-Hill, 1961.